GEOPHYSICS, VOL. 70, NO. 2 (MARCH-APRIL 2005); P. D1–D8, 7 FIGS.
10.1190/1.1897026

Parameter estimation in orthorhombic media using multicomponent wide-azimuth reflection data

Vladimir Grechka[1], Andrés Pech[2], and Ilya Tsvankin[2]

ABSTRACT

Orthorhombic models with a horizontal symmetry plane adequately describe seismic signatures recorded over many naturally fractured reservoirs. The inversion of wide-azimuth traveltimes of PP and SS (the fast S_1 and slow S_2) reflections are discussed for Tsvankin's anisotropic parameters and the azimuths of the vertical symmetry planes of orthorhombic media. If shear waves are not excited, SS traveltimes can be found from PP and PS (converted-wave) data, which makes the method applicable to offshore surveys.

The feasibility of parameter estimation is strongly dependent on reflector dip and orientation. For a horizontal reflector beneath a single orthorhombic layer, the vertical velocities and reflector depth cannot be found from conventional-spread reflection traveltimes alone. If the reflector is dipping, the inversion is ambiguous when the dip plane is close to one of the vertical symmetry planes of the orthorhombic layer above it. The parameter estimation becomes possible if the dip direction deviates by more than 10° from the nearest symmetry plane.

We apply multicomponent stacking velocity tomography to perform velocity analysis for stratified orthorhombic models composed of homogeneous layers separated by plane or curved interfaces. The tomographic algorithm, which operates with the normal-moveout (NMO) ellipses, zero-offset traveltimes, and reflection time slopes of PP- and SS-waves, is designed to build the orthorhombic velocity model in the depth domain by estimating the anisotropic parameters and the shapes of the reflecting interfaces. Numerical tests show that for layered orthorhombic media, it is necessary to put constraints on the vertical velocities to avoid instability in the inversion of noise-contaminated reflection data.

INTRODUCTION

Estimation of anisotropic velocity fields from reflection traveltimes of seismic waves is a nonlinear inverse problem that becomes increasingly more complicated for lower medium symmetries. The existence of a unique solution is determined by the reflection mode (PP, SS, PS, or a certain combination of them) being used, the available range of offsets and azimuths, and the reflector geometry.

For the simplest anisotropic model — transverse isotropy with a vertical symmetry axis (VTI) — PP-waves alone generally do not provide enough information for estimating Thomsen anisotropic parameters ϵ and δ. If the VTI medium above the reflector is laterally homogeneous, PP traveltimes are fully controlled by the NMO (normal-moveout) velocity $V_{\rm nmo}(0)$ and the anellipticity coefficient η, rather than by the vertical P-wave velocity V_{P0}, ϵ, and δ individually (Alkhalifah and Tsvankin, 1995; Grechka and Tsvankin, 1998a, b). It is possible to invert PP traveltimes for a limited class of VTI models with dipping or curved intermediate interfaces for the interval values of V_{P0}, ϵ, and δ (Le Stunff et al., 2001; Grechka et al., 2002a). Supplementing PP moveout data with converted PSV-waves overcomes the ambiguity in the inversion for the vertical velocities, ϵ and δ, provided the reflector has a mild dip (Tsvankin and Grechka, 2000a, b; Tsvankin, 2001). It is even more essential to combine PP and PS (in general, there are two split converted waves: PS_1 and PS_2) data in parameter estimation for lower symmetry models, such as orthorhombic and monoclinic (Grechka et al., 1999, 2000).

Unfortunately, processing of converted waves (e.g., Granli et al., 1999) is complicated by a number of practical problems related to polarity reversals, conversion-point dispersal, and

Manuscript received by the Editor February 4, 2003; revised manuscript received December 22, 2003; published online March 22, 2005.
[1]Formerly Colorado School of Mines, Center for Wave Phenomena, Department of Geophysics, Golden, Colorado 80401-1887; presently Shell International Exploration and Production Incorporated, Bellaire Technology Center, 3737 Bellaire Boulevard, Houston, Texas 77001-0481. E-mail: Vladimir.grechka@shell.com.
[2]Colorado School of Mines, Center for Wave Phenomena, Department of Geophysics, Golden, Colorado 80401-1887. E-mail: andrespech@yahoo.com; ilya@dix.mines.edu.

the asymmetry of PS-wave moveout on common-midpoint (CMP) and common-conversion-point (CCP) gathers. In particular, velocity-analysis algorithms based on the conventional hyperbolic moveout equation cannot handle asymmetric PS moveout (see the discussion of "diodic" velocity in Thomsen, 1999). These difficulties in converted-wave processing can be overcome using a method proposed by Grechka and Tsvankin (2002) and Grechka and Dewangan (2003). Grechka and Tsvankin (2002) showed that the traveltimes of PP and PS reflections from a certain interface can be combined to obtain the traveltimes of pure (nonconverted) SS-waves for the same reflector. Most important, SS traveltimes can be computed without precise velocity information, so the whole procedure can be performed prior to anisotropic velocity analysis (although it is necessary to correlate PP and PS reflections).

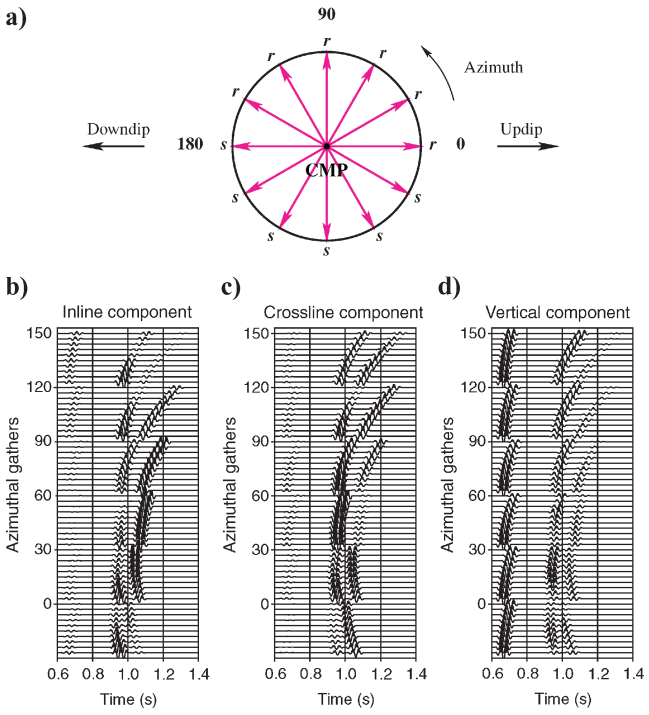

Figure 1. (a) Plan view of a multiazimuth CMP gather, with sources (a vertical force at the free surface) located on the side marked by *s*, and receivers on the side marked by *r*. (b–d) True-amplitude, three-component synthetic seismograms of PP-, PS_1-, and PS_2-waves reflected from a dipping interface beneath an orthorhombic layer. The numbers 0, 30, 60, 90, 120, and 150 on the vertical axis in (b–d) indicate the azimuth (in degrees) for the block of traces plotted under this number (e.g., all traces between numbers 150 and 120 are recorded on the CMP line with the azimuth 150°). The source-receiver offsets for each block of traces (i.e., CMP line) change from 0.1 km to 1 km in 0.1 km increments. The azimuth of the dip plane is $\psi = 0^\circ$ (see the plan view), the dip $\phi = 30^\circ$, and the depth under the common midpoint $z = 1$ km. The azimuth of the vertical $[x_1, x_3]$ symmetry plane of the orthorhombic layer with respect to the reflector dip plane is $\beta = 60^\circ$. Tsvankin's (1997) parameters of the layer are $V_{P0} = 2.9$ km/s, $V_{S0} = 1.4$ km/s, $\epsilon^{(2)} = 0.15$, $\delta^{(2)} = 0.05$, $\gamma^{(2)} = -0.25$, $\epsilon^{(1)} = 0.25$, $\delta^{(1)} = 0.15$, $\gamma^{(1)} = -0.20$, $\delta^{(3)} = -0.05$; the density $\rho = 1.9$ g/cm^3. The reflecting half-space is isotropic with the P-wave velocity $V_P = 3.0$ km/s, S-wave velocity $V_S = 1.5$ km/s, and density $\rho = 2.1$ g/cm^3.

While the original formulation of the method requires traveltime picking, Grechka and Dewangan (2003) demonstrated that SS data can be generated by a specially designed convolution of windowed PP and PS seismograms. The computed SS arrivals are called pseudo–SS data because they have the correct traveltimes but not amplitudes of the primary SS reflections. Processing of the SS-waves constructed from PP and PS data yields SS-wave NMO velocities (in 2D) or NMO ellipses (in 3D), which can be combined with PP moveout in anisotropic parameter estimation.

A practical velocity-analysis technique based on these ideas was suggested for transversely isotropic media with a vertical and tilted axis of symmetry by Grechka et al. (2002b). They used the NMO ellipses, zero-offset traveltimes, and reflection time slopes of PP- and SS(SVSV)-waves as input to a tomographic inversion algorithm (stacking-velocity tomography) capable of estimating the interval anisotropic parameters and the shapes of layer boundaries. Grechka et al. (2002c) successfully applied this method to anisotropic parameter estimation at the Siri reservoir in the North Sea.

Next, we discuss the inversion of multicomponent reflection data for more complicated orthorhombic media believed to be typical for naturally fractured oil and gas reservoirs (Wild and Crampin, 1991; Schoenberg and Helbig, 1997; Bakulin et al., 2000). The main goal of this article is to develop a practical velocity-analysis algorithm for building orthorhombic models in the depth domain using wide-azimuth reflection traveltimes of PP-waves and two split converted waves (PS_1 and PS_2). First, we establish the conditions that make it possible to estimate the vertical velocities and Tsvankin's (1997) anisotropic coefficients of a single orthorhombic layer above a dipping reflector. Then, we extend multicomponent stacking-velocity tomography to models composed of multiple homogeneous orthorhombic layers separated by plane or curved interfaces. Although for a certain class of such layered media, the inversion of multicomponent data is theoretically possible, it may not be sufficiently stable without constraints on the vertical velocities.

TOMOGRAPHIC PARAMETER ESTIMATION USING MULTICOMPONENT DATA

The success of the parameter-estimation procedure discussed below depends on our ability to obtain SS traveltimes from PP and PS reflection data using the method of Grechka and Tsvankin (2002) and Grechka and Dewangan (2003). Although this method requires no explicit velocity information, one must be able to identify and correlate PP and PS reflections from the same interface on prestack data. Then, the convolutional technique of Grechka and Dewangan (2003) can be applied to windowed PP and PS traces to compute SS data suitable for moveout velocity analysis. Identification of PS arrivals, however, may be difficult for traces with low PS amplitudes (and, correspondingly, low S/N ratio) caused by small reflection coefficients in areas of polarity reversals. To evaluate the seriousness of this issue for a typical, moderately anisotropic orthorhombic model, a synthetic test is used.

The multicomponent seismograms in Figure 1 are computed by anisotropic dynamic ray tracing (Obolentseva and Grechka, 1989) for a single orthorhombic layer with a dipping lower boundary. As expected, the PP reflection has the highest

amplitude on the vertical component (Figure 1d), whereas the two split converted waves PS_1 and PS_2 are clearly seen on the horizontal inline and crossline components (Figures 1b, c). Although we observe some dimming of the PS_1- and PS_2-waves at certain azimuths, the offset range of those low-amplitude arrivals is relatively narrow. Therefore, Figure 1 suggests that, despite the presence of polarity reversals, converted-wave reflections over orthorhombic media can be efficiently used for generating SS data. This conclusion remains valid for models with a smaller shear-wave splitting coefficient where PS_1 and PS_2 arrivals overlap, and it is necessary to apply Alford (1986) rotation.

Once PP, PS_1, and PS_2 arrivals have been correlated, the method of Grechka and Tsvankin (2002) and Grechka and Dewangan (2003) can be employed to compute seismograms of the shear-wave reflections S_1S_1 and S_2S_2 from the same interface. The traveltimes t_{S1} and t_{S2} of these pure shear waves are guaranteed to be symmetric with respect to the common midpoint so they can be processed by means of hyperbolic semblance analysis. For wide-azimuth data, it is possible to reconstruct the NMO ellipses of both PP- and SS-waves using a 3D hyperbolic semblance operator (Grechka and Tsvankin, 1999b).

The NMO ellipses, along with the corresponding horizontal projections $\mathbf{p}_Q$ of the slowness vectors (the reflection slopes on zero-offset time sections) and zero-offset traveltimes τ_Q (Q = P, S_1, or S_2), are used as the input data for anisotropic stacking-velocity tomography. The data vector for an N-layered orthorhombic medium is

$$\mathbf{d}(Q, \mathbf{Y}, n) \equiv \{\tau_Q(\mathbf{Y}, n), \mathbf{p}_Q(\mathbf{Y}, n), \mathbf{W}_Q(\mathbf{Y}, n)\}, \qquad (1)$$

where $\mathbf{Y} = [Y_1, Y_2]$ is the CMP location, $n = 1, 2, \ldots, N$ is the reflector number and $\mathbf{W}$ is the 2×2 matrix (Grechka and Tsvankin, 1998b) that describes the NMO ellipse.

Stacking-velocity tomography for multicomponent data is described in detail by Grechka et al. (2002b). One of the main advantages of restricting the inversion to the hyperbolic portion of reflection moveout is high computational efficiency because the NMO ellipse for a given reflection event can be computed by tracing only one (zero-offset) ray. Also, NMO ellipses provide valuable analytic insight into the constrained parameter combinations (Grechka et al., 2002a, b).

The tomographic algorithm is based on a two-step procedure for estimating the model vector $\mathbf{m}$ that contains the interval parameters of orthorhombic media and the coefficients of the polynomials specifying the model interfaces. First, for a given set of trial interval anisotropic parameters, the zero-offset traveltimes and reflection slopes are used to compute the one-way zero-offset rays and reconstruct the medium interfaces (i.e., build the trial model in depth). Second, the NMO ellipses $\mathbf{W}$ are calculated in the trial model for all recorded reflection PP and SS events at each CMP location. Then the interval parameters are updated according to the misfit between the calculated and measured NMO ellipses, and the minimization procedure continues as described above.

In the next section, we discuss the issues of uniqueness and stability in the inversion of the data vector 1 for the parameters of orthorhombic media.

PARAMETER ESTIMATION IN A SINGLE ORTHORHOMBIC LAYER

We briefly review notation and some relevant properties of wave propagation for orthorhombic models. Seismic signatures in orthorhombic media can be conveniently described in terms of the vertical velocities of P-waves and one of the split S-waves (V_{P0} and V_{S0}, respectively) and Thomsen-style anisotropic coefficients $\epsilon^{(1,2)}$, $\delta^{(1,2,3)}$, and $\gamma^{(1,2)}$ introduced by Tsvankin (1997). The coefficients $\epsilon^{(i)}$, $\delta^{(i)}$, $\gamma^{(i)}$ ($i = 1, 2$) are defined in the vertical symmetry planes $[x_2, x_3]$ and $[x_1, x_3]$ (Figure 2), and have the same meaning as Thomsen's (1986) parameters ϵ, δ, and γ for transverse isotropy. The coefficient $\delta^{(3)}$ plays the role of Thomsen's δ in the horizontal plane $[x_1, x_2]$. Here, the superscript (1, 2, or 3) denotes the axis orthogonal to the plane where the coefficient is defined. For more details, see Tsvankin (1997, 2001).

The kinematics of wave propagation in the symmetry planes of orthorhombic media is practically identical to that in VTI media. The only notable difference is caused by the so-called singularity directions in orthorhombic media (point A in Figure 2), where the phase velocities of two shear waves coincide. The S_2-wavefront near a singularity usually becomes multivalued, while the wavefront of the fast mode S_1 develops an elliptical hole. Those complicated phenomena are outside the scope of this article; we assume, hereafter, that there are no singularities inside the fan of ray directions used for velocity analysis.

Horizontal reflector

The axes of the NMO ellipses for all reflection modes in a horizontal orthorhombic layer are co-oriented with the vertical symmetry planes (Grechka et al., 1999):

$$\frac{1}{V^2_{\mathrm{nmo},Q}(\alpha)} = \frac{\cos^2\alpha}{\left[V^{(2)}_{\mathrm{nmo},Q}\right]^2} + \frac{\sin^2\alpha}{\left[V^{(1)}_{\mathrm{nmo},Q}\right]^2} \qquad (Q = P, S_1, \text{or } S_2); \quad (2)$$

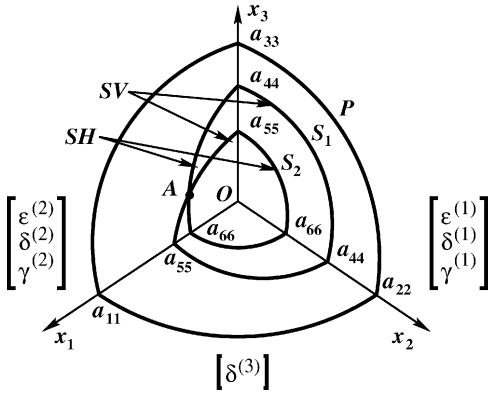

Figure 2. Sketch of body-wave phase-velocity surfaces in orthorhombic media (after Grechka et al., 1999). The coefficients $\epsilon^{(1)}$, $\delta^{(1)}$, and $\gamma^{(1)}$ are defined in the symmetry plane $[x_2, x_3]$, while $\epsilon^{(2)}$, $\delta^{(2)}$, and $\gamma^{(2)}$ correspond to the plane $[x_1, x_3]$ (Tsvankin, 1997). The vertical velocity V_{S0} is computed for the S-wave polarized in the x_1-direction. $a_{ij} \equiv \sqrt{c_{ij}/\rho}$, where c_{ij} are the stiffness coefficients and ρ is the density. Point A marks a shear-wave singularity.

α is the azimuth with respect to the $[x_1, x_3]$-plane. Because of the kinematic equivalence between the symmetry planes of orthorhombic and VTI media, the semi-axes of the NMO ellipses ($V^{(i)}_{\mathrm{nmo},Q}$) can be obtained by adapting the VTI equations (Grechka and Tsvankin, 1998b). Assuming that the fast mode S_1 at vertical incidence is polarized in the x_2-direction yields (Grechka et al., 1999),

$$V^{(2)}_{\mathrm{nmo},P} = V_{P0}\sqrt{1+2\delta^{(2)}}, \tag{3}$$

$$V^{(1)}_{\mathrm{nmo},P} = V_{P0}\sqrt{1+2\,\delta^{(1)}}, \tag{4}$$

$$V^{(2)}_{\mathrm{nmo},S1} = V_{S1}\sqrt{1+2\gamma^{(2)}} = \sqrt{c_{66}/\rho}, \tag{5}$$

$$V^{(1)}_{\mathrm{nmo},S1} = V_{S1}\sqrt{1+2\sigma^{(1)}}, \tag{6}$$

$$V^{(2)}_{\mathrm{nmo},S2} = V_{S2}\sqrt{1+2\sigma^{(2)}}, \tag{7}$$

$$V^{(1)}_{\mathrm{nmo},S2} = V_{S2}\sqrt{1+2\,\gamma^{(1)}} = \sqrt{c_{66}/\rho}, \tag{8}$$

where

$$\sigma^{(1)} \equiv \left(\frac{V_{P0}}{V_{S1}}\right)^2 \left(\epsilon^{(1)} - \delta^{(1)}\right),$$

$$\sigma^{(2)} \equiv \left(\frac{V_{P0}}{V_{S2}}\right)^2 \left(\epsilon^{(2)} - \delta^{(2)}\right). \tag{9}$$

V_{S1} and V_{S2} are the vertical velocities of the fast and slow shear-waves (respectively), which can be expressed as

$$V_{S1} = V_{S0}\sqrt{\frac{1+2\gamma^{(1)}}{1+2\gamma^{(2)}}}, \qquad V_{S2} = V_{S0}. \tag{10}$$

As follows from equations 3 through 10, the anisotropic coefficients $\epsilon^{(1,2)}$, $\delta^{(1,2)}$, and $\gamma^{(1,2)}$ can be estimated in a unique fashion only if either one of the vertical velocities or the reflector depth is known. This result is hardly surprising because the NMO velocities and zero-offset traveltimes cannot be unambiguously inverted for the anisotropic parameters even for the higher-symmetry horizontal VTI layer.

Note that the coefficient $\delta^{(3)}$ has no influence on the NMO ellipses in a horizontal layer and, therefore, cannot be determined from conventional-spread reflection moveout. A more detailed discussion of the NMO ellipses of pure and converted waves in horizontally layered orthorhombic media, and their inversion, can be found in Grechka et al. (1999).

Plane-dipping reflector co-oriented with a vertical symmetry plane

While moveout inversion of multicomponent data is nonunique for a horizontal VTI layer, Tsvankin and Grechka (2000a, b) and Grechka et al. (2002b) showed that the vertical velocities and coefficients ϵ and δ can be estimated uniquely from PP and SS traveltimes if the reflector beneath the VTI medium has a mild dip of at least 15–20°. We examine whether or not this result holds for an orthorhombic layer above a plane-dipping reflector that is oriented so that the dip plane coincides with one of the vertical symmetry planes of the overburden.

Suppose the dip plane of the reflector represents the $[x_1, x_3]$ symmetry plane of the orthorhombic medium. Since the slowness vector of the zero-offset ray for any pure mode is orthogonal to the reflector, the horizontal slowness projection at zero offset is confined to the dip plane. In general, both horizontal slowness components (p_1 and p_2) of the zero-offset ray can be found from reflection slopes on the zero-offset (or stacked) time section (Grechka and Tsvankin, 1998b). Therefore, reflection time slopes can be used to determine the azimuthal direction of the reflector and of the $[x_1, x_3]$ symmetry plane.

The model vector $\mathbf{m}$ to be estimated from moveout data contains the remaining eleven unknowns: nine Tsvankin's (1997) parameters discussed above (V_{P0}, V_{S0}, $\epsilon^{(1)}$, $\epsilon^{(2)}$, $\delta^{(1)}$, $\delta^{(2)}$, $\delta^{(3)}$, $\gamma^{(1)}$, and $\gamma^{(2)}$), the reflector dip ϕ, and the distance D between the reflector and the origin $\mathbf{O}$ of the Cartesian coordinate system. The elements of $\mathbf{m}$ are supposed to be found from the 18-component data vector 1 that has six zero elements,

$$p_{2,Q} = 0 \quad \text{and} \quad W_{12,Q} = 0 \quad (Q = P, S_1, \text{or } S_2), \tag{11}$$

because $[x_1, x_3]$ is the symmetry plane for the model as a whole. The remaining elements — three zero-offset traveltimes τ_Q, three horizontal slownesses $p_{1,Q}$, and six diagonal elements of the matrices $\mathbf{W}_Q$ (which correspond to the dip- and strike-components of the NMO velocities) — provide a total of 12 equations.

However, below we demonstrate that the expressions for the traveltimes τ_Q are not independent. The equation of a planar reflector can be written as

$$\mathbf{n}\cdot\mathbf{x} = D, \tag{12}$$

where $\mathbf{n} \equiv [\sin\phi, 0, \cos\phi]$ is a unit vector perpendicular to the reflector. Assuming that the origin $\mathbf{O}$ of the Cartesian coordinate system is placed at the common midpoint, the reflection point $\mathbf{r}_Q$ of the zero-offset ray can be found from

$$\mathbf{r}_Q = \mathbf{g}_Q\tau_Q, \tag{13}$$

where $\mathbf{g}_Q$ is the group-velocity vector of mode Q = P, S_1, or S_2. Since the point $\mathbf{r}_Q$ lies on the reflector 12, the one-way zero-offset traveltime is

$$\tau_Q = \frac{D}{\mathbf{n}\cdot\mathbf{g}_Q}. \tag{14}$$

Snell's law requires that the slowness vectors $\mathbf{p}_Q \equiv [p_{1,Q}, 0, p_{3,Q}]$ of pure-mode zero-offset reflections be orthogonal to the reflector; therefore,

$$\mathbf{n} = \frac{\mathbf{p}_Q}{|\mathbf{p}_Q|}. \tag{15}$$

Combining equations 14 and 15 and taking into account that $\mathbf{p}_Q\cdot\mathbf{g}_Q = 1$ (this equality plays the role of eikonal equation in anisotropic media) yields

$$\tau_Q = \frac{D|\mathbf{p}_Q|}{\mathbf{p}_Q\cdot\mathbf{g}_Q} = D|\mathbf{p}_Q| = \frac{Dp_{1,Q}}{\sin\phi} \qquad (Q = P, S_1, \text{or } S_2). \tag{16}$$

Equation 16 shows that the three zero-offset traveltimes (τ_P, τ_{S1}, and τ_{S2}) constrain only one combination of the model parameters ($D/\sin\phi$). Therefore, the number of independent equations to be solved for the 11 unknown parameters reduces from 12 to 10. Clearly, this inverse problem does not have a unique solution.

Arbitrarily oriented plane-dipping reflector

If the dip plane of the reflector does not coincide with either vertical symmetry plane, each NMO ellipse generally has a different orientation. That increases the number of independent components of the data vector 1 and, as demonstrated below, can make the inversion unambiguous.

If the dip plane and the symmetry planes are misaligned, the number of equations exceeds the number of unknowns. The model vector includes 13 elements to be found from the data,

$$\mathbf{m} = \{V_{P0}, V_{S0}, \epsilon^{(1)}, \delta^{(1)}, \gamma^{(1)}, \epsilon^{(2)}, \delta^{(2)}, \gamma^{(2)}, \delta^{(3)}, D, \phi, \psi, \beta\}, \quad (17)$$

where ϕ, as before, is the reflector dip, ψ is the azimuth of the dip plane of the reflector, and β is the azimuth of the vertical symmetry plane $[x_1, x_3]$ with respect to the axis Y_1 of the observational coordinate frame. The original number of equations (i.e., the number of measured quantities) is 18 (equation 1) but, as discussed previously, the three traveltimes τ_Q provide only one independent equation (equation 16 remains valid for any reflector orientation). In addition, the ratio of the horizontal slowness components for each mode is fixed by the reflector azimuth ($p_{2,Q}/p_{1,Q} = \tan\psi$), which eliminates two more independent equations. Even with these factors taken into account, the number of equations 14 is larger than the number of unknown model parameters 13, and, in principle, the moveout inversion may be possible.

Still, the inverse problem is nonlinear, and the feasibility of parameter estimation has to be assessed by numerical testing on noise-contaminated data. Our numerical analysis shows that the inversion for a range of typical orthorhombic models is not only unique but also quite stable. Because of the multimodal nature of the misfit function, we perform several inversions starting from different points in the model space. The results in Figure 3 are obtained from the data $\mathbf{d} = \{\tau_Q, \mathbf{p}_Q, \mathbf{W}_Q\}$ generated for all three modes (P, S_1, and S_2) at a single CMP location. The traveltimes τ_Q, the horizontal slowness components $\mathbf{p}_Q$, and the NMO ellipses $\mathbf{W}_Q$ were contaminated by Gaussian noise with standard deviations of 1% for τ_Q and $\mathbf{p}_Q$ and 2% for $\mathbf{W}_Q$. (These values of standard deviations may be considered as typical for traveltimes and moveout velocities obtained from semblance analysis.)

The parameter estimation was repeated 100 times for different realizations of the noise using a nonlinear least-squares algorithm. The maximum standard deviation in the recovered anisotropic coefficients does not exceed 0.025 (the value for $\delta^{(1)}$ in Figure 3), which means that the inversion is sufficiently stable. The standard deviations for the parameters not displayed in Figure 3 are small as well (see the figure caption).

For the model from Figure 3, the dip plane of the reflector deviates by 30° from the nearest vertical symmetry plane, which ensures the high stability of the inversion result. Figure 4 shows the inversion output for a model similar to that in Figure 3, but the azimuthal angle between the dip plane and a vertical symmetry plane is just 15°, and the dip ϕ is reduced from 30° to 20°. Both changes have a negative influence on the performance of the inversion algorithm, and the error bars for most parameters become noticeably longer. Still, the moderate magnitude of the standard deviations indicates that the inversion remains sufficiently stable for practical applications.

Further reduction in the difference $|\psi - \beta|$ or in the reflector dip leads to a rapid increase in the errors (i.e., in the standard deviations). Indeed, the analysis in the previous section proves that the inversion becomes nonunique when $|\psi - \beta|$ approaches $k\pi/2$ ($k = 0, \pm1, \pm2, \ldots$). Numerical testing shows that stable application of this algorithm requires the dip direction to deviate from the nearest symmetry plane by more than 10°.

Likewise, the inversion becomes unstable if the reflector dip $\phi < 15°$, and for subhorizontal reflectors the anisotropic coefficients cannot be estimated without a priori knowledge of the vertical velocities or reflector depth (see above). A similar dependence of the quality of moveout-inversion results on reflector dip was found for multicomponent data in VTI media by Tsvankin and Grechka (2000a, b) and Grechka et al. (2002b).

Curved reflector

If the reflector beneath an orthorhombic layer has spatially varying curvature, the uniqueness of the inversion procedure is even more difficult to evaluate analytically. The feasibility of estimating the medium parameters in this case strongly depends on the shape and parameterization of the reflector and the spatial distribution of the common midpoints. Grechka

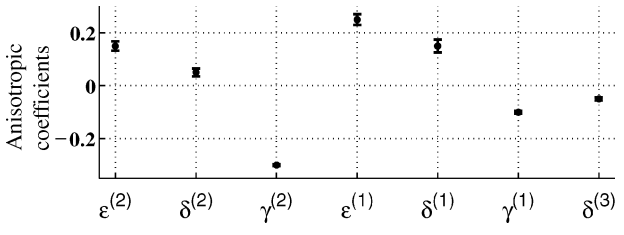

Figure 3. Inversion results for a single orthorhombic layer above a dipping reflector. The exact values of the anisotropic coefficients are marked by the dots; the bars correspond to the ± standard deviation in each parameter. The reflector dip ϕ is 30°, the azimuth of the dip plane of the reflector $\psi = 0°$, and the azimuth of the $[x_1, x_3]$ symmetry plane of the layer $\beta = 60°$. The standard deviations for the parameters not shown on the plot are 1.2% and 0.6% for the velocities V_{P0} and V_{S0}, respectively, and less than 1° for the angles ϕ, ψ, and β.

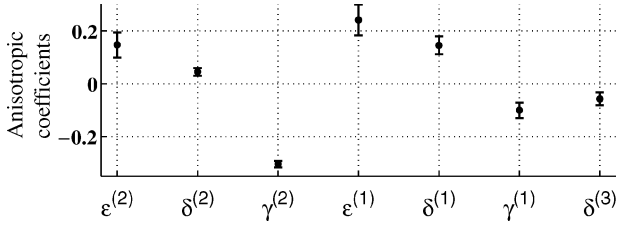

Figure 4. Same as Figure 3, but the reflector dip ϕ is 20°, and the azimuth of the $[x_1, x_3]$ symmetry plane $\beta = 15°$ (the azimuth of the dip plane remains $\psi = 0°$). The standard deviations for the parameters not shown on the plot are 1.3% and 0.7% for the velocities V_{P0} and V_{S0}, respectively, and less than 1.5° for the angles ϕ, ψ, and β.

et al. (2002a) discussed those issues for stacking-velocity tomography of P-waves in VTI media.

Extensive testing on synthetic traveltimes shows that reflector curvature does not pose any serious problems for the parameter estimation in a single orthorhombic layer, provided the reflecting interface contains dips over 15° and the dip directions deviate from the vertical symmetry planes. Typical inversion results for noise-contaminated data $\{\tau_Q, \mathbf{p}_Q, \mathbf{W}_Q\}$ from nine CMP locations are displayed in Figure 5. As in the previous test, the inversion was repeated 100 times to study the distribution of the estimated parameters. The standard deviations in Figure 5b are even smaller than those in Figure 3; this conclusion also holds for the vertical velocities V_{P0}, V_{S0}, and the reflector orientation (not shown).

The increase in the stability of the inversion algorithm for the curved reflector in Figure 5 is explained by the relatively wide range of reflector dips and azimuths sampled by the zero-offset rays. In other words, each CMP provides independent information. This advantage of curved interfaces, of course, can be fully exploited only if it is still possible to treat the medium above the reflector as homogeneous.

STACKING-VELOCITY TOMOGRAPHY IN LAYERED MEDIA

The above analysis for a single orthorhombic layer helped to reveal the potential of the multicomponent inversion algorithm. In this section, the methodology of stacking-velocity tomography is applied to more realistic models composed of homogeneous orthorhombic layers separated by plane or curved interfaces.

If noise-free data $\{\tau_Q, \mathbf{p}_Q, \mathbf{W}_Q\}$ ($Q = P, S_1, S_2$) for all interfaces are available, and the reflectors satisfy the conditions established for a single layer (i.e., the dips exceed 15–20° and the reflector azimuths deviate by more than 10° from those of the vertical symmetry planes), the tomographic algorithm can recover the interval orthorhombic parameters along with the shapes of the interfaces. However, because of error accumulation with depth and a lower sensitivity of surface data to the parameters of deeper layers (e.g., Grechka et al., 2002a), even moderate noise may cause substantial errors in the interval parameters.

To make the inversion more stable for field-data applications, we put constraints on the interval vertical velocities ($V_{P0,n}$ or $V_{S0,n}$) in all layers $n = 1, \ldots, N$; alternatively, it is possible to constrain the thickness of each layer. Such an assumption may not be overly restrictive in reservoir characterization because seismic inversion for orthorhombic anisotropy would typically be performed at later stages of the reservoir development when borehole and check-shot data are already available.

Figure 6 shows the parameter-estimation results for a model composed of three horizontal orthorhombic layers. The data

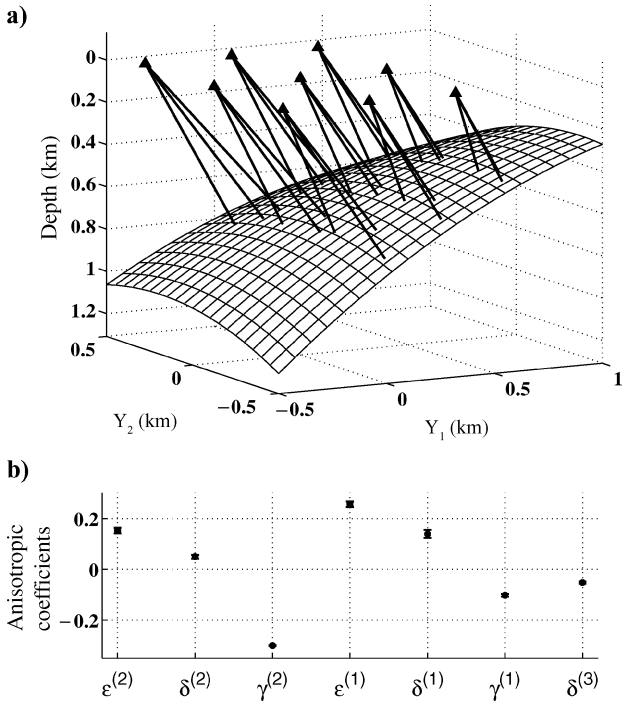

Figure 5. (a) Zero-offset rays of the P-, S_1-, and S_2-waves reflected from a curved interface below an orthorhombic layer and (b) the estimated anisotropic coefficients. The $[x_1, x_3]$ symmetry plane makes an angle of 60° with the Y_1-axis. Tsvankin's (1997) medium parameters and the standard deviations of the Gaussian noise are the same as those in Figure 3.

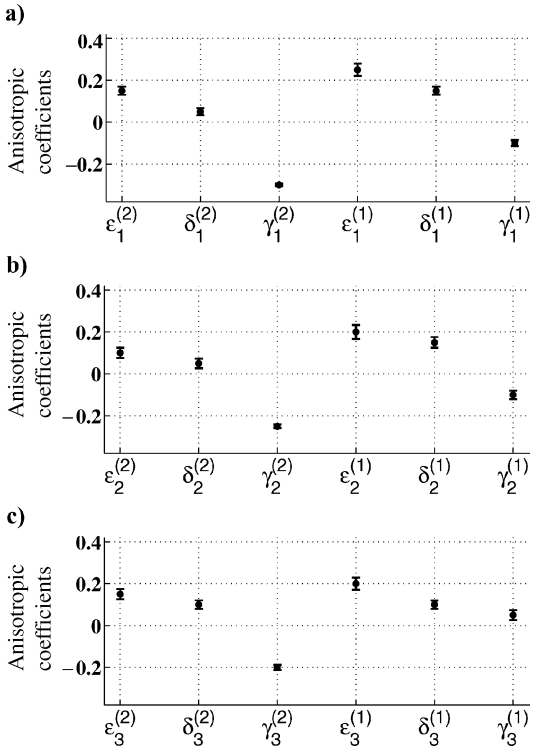

Figure 6. The results of stacking-velocity tomography for a model composed of three horizontal layers — (a) top layer, (b) middle layer, (c) bottom layer — with different azimuths of the vertical symmetry planes. The vertical velocities were constrained to be within ±3% of the correct values; from top to bottom, $V_{P0,1} = 1.0$ km/s, $V_{S0,1} = 0.5$ km/s, $V_{P0,2} = 1.5$ km/s, $V_{S0,2} = 0.6$ km/s, and $V_{P0,3} = 1.8$ km/s, $V_{S0,3} = 1.0$ km/s. The layer thicknesses are $z_1 = 0.4$ km, $z_2 = 0.6$ km, and $z_3 = 0.8$ km, and the azimuths of the symmetry plane $[x_1, x_3]$ are $\beta_1 = 40°$, $\beta_2 = 70°$, and $\beta_3 = 10°$.

$\{\tau_Q, \mathbf{p}_Q, \mathbf{W}_Q\}$ were generated for nine common midpoints and contaminated by Gaussian noise with standard deviations of 1% for the zero-offset traveltimes τ_Q and horizontal slownesses $\mathbf{p}_Q$ and 2% for the matrices $\mathbf{W}_Q$ describing the NMO ellipses. Since the inversion for layer-cake models requires information about the vertical velocities or reflector depth (Grechka et al., 1999), the interval velocities $V_{P0,n}$, $V_{S0,n}$ ($n = 1, 2, 3$) were allowed to deviate by no more than ±3% from the correct values. The results in Figure 6 indicate that all interval anisotropic coefficients except for $\delta^{(3)}$ are estimated with high accuracy (the standard deviations do not exceed 0.03), and the standard deviations in the azimuths of the symmetry planes are less than 1.5°. As discussed above, the parameter $\delta^{(3)}$ has no influence on the NMO ellipses of P- and S-waves in a horizontal orthorhombic layer; therefore, it cannot be determined from the input data. Note, however, that $\delta^{(3)}$ contributes to nonhyperbolic reflection moveout and potentially can be constrained using long-offset traveltimes.

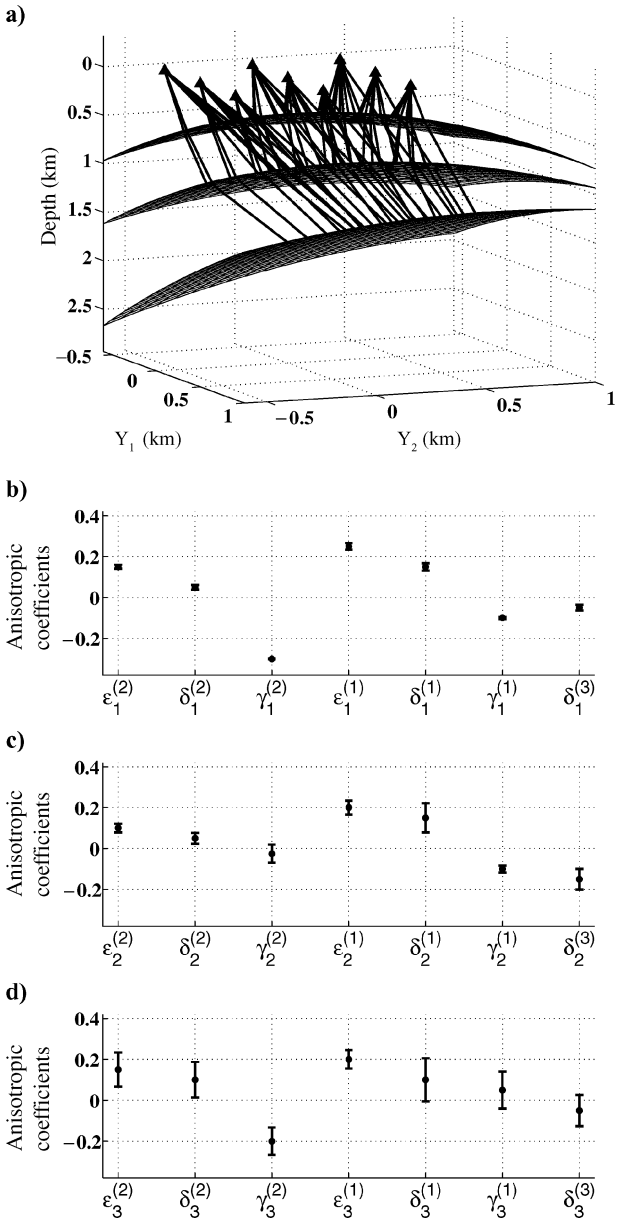

Figure 7. (a) Reflected zero-offset rays of the P-, S_1-, and S_2-waves in a three-layer orthorhombic medium and (b–d) the results of stacking-velocity tomography. The vertical velocities ($V_{P0,1} = 1.0$ km/s, $V_{S0,1} = 0.6$ km/s, $V_{P0,2} = 1.5$ km/s, $V_{S0,2} = 0.8$ km/s, and $V_{P0,3} = 1.8$ km/s, $V_{S0,3} = 1.0$ km/s) were assumed to be known. The azimuths of the symmetry plane $[x_1, x_3]$ are $\beta_1 = 40°$, $\beta_2 = 50°$, and $\beta_3 = 10°$.

Application of our tomographic algorithm to a more complicated layered model with curved interfaces is illustrated in Figure 7. The input data were computed again for nine common midpoints (Figure 7a) and contaminated by Gaussian noise with the same standard deviations as those in Figure 6. The vertical velocities in all three layers were fixed at the correct values.

In addition to the interval anisotropic parameters and the azimuths β_n of the vertical symmetry planes, the algorithm was designed to reconstruct the shapes of all three interfaces. As expected for any technique based on surface traveltime data, parameter estimation becomes less stable with depth (Figures 7b–d). Nevertheless, the standard deviations in the anisotropic parameters do not exceed 0.1 (the value for $\delta_3^{(1)}$ in Figure 7d). Taking into account that the error amplification for a given layer is proportional to its thickness normalized by depth, we conclude that the anisotropic coefficients are constrained reasonably well. The azimuths of the symmetry planes and the shapes of the interfaces were also estimated with high accuracy; the standard deviations in β_1, β_2, and β_3 are 1.0°, 1.6°, and 4.6°, respectively.

DISCUSSION AND CONCLUSIONS

Estimating the parameters of orthorhombic media from surface seismic data is of primary importance in characterization of naturally-fractured reservoirs. We demonstrated that for a range of orthorhombic models, 3D multiazimuth-reflection moveout of PP-waves and two split SS-waves on conventional length spreads can help to reconstruct the velocity field in the depth domain. Reflection SS data can be generated from PP-waves and converted PS-waves prior to anisotropic velocity analysis using the method of Grechka and Tsvankin (2002) and Grechka and Dewangan (2003), so excitation of shear waves is not necessary. Note that although this method does not require explicit velocity information, PP and PS events have to be correlated on prestack gathers. Then the NMO ellipses, zero-offset traveltimes, and reflection slopes of the PP- and SS-waves are inverted for the interval anisotropic parameters and the shapes of the interfaces (we call this technique, stacking-velocity tomography).

To avoid ambiguity in the inversion for a single orthorhombic layer, the reflector needs to have at least a mild dip ϕ, and the azimuth of the dip plane of the reflector has to be sufficiently different from that of the nearest vertical symmetry plane of the overburden. If the reflector is horizontal ($\phi = 0°$), the vertical velocities and the anisotropic parameters $\epsilon^{(1,2)}$, $\delta^{(1,2,3)}$, and $\gamma^{(1,2)}$ cannot be obtained from the reflection traveltimes of PP- and SS-waves (or PS-waves) alone (Grechka et al., 1999). Even a mild reflector dip $\phi = 15$–$20°$, however, makes the inversion for a single orthorhombic layer feasible (subject to the condition discussed below); a similar result

was obtained by Tsvankin and Grechka (2000a, b) for VTI media.

When the dip plane of the reflector represents one of the vertical symmetry planes of the overburden, the NMO ellipses are co-oriented with the dip and strike directions and do not contain enough information about the medium parameters. The deviation of the dip direction from the nearest symmetry plane has to exceed 10° to ensure unambiguous inversion. It should be mentioned that the inversion of multiazimuth PP-wave traveltimes for the anellipticity parameters $\eta^{(1,2,3)}$ of orthorhombic media also breaks down when the dip plane of the reflector is aligned with a vertical symmetry plane of the medium (Grechka and Tsvankin, 1999a).

A number of synthetic tests on noise-contaminated data for typical orthorhombic models shows that, for a single layer, noise does not get amplified by the inversion algorithm. In contrast, the estimated anisotropic parameters in layered orthorhombic media often are significantly distorted as a result of error accumulation with depth and a reduced sensitivity of surface data to the parameters of deeper layers. Constraining the vertical velocities using well logs or (vertical seismic profiling) VSP data removes this instability in stacking-velocity tomography and makes the inversion results suitable for application in quantitative fracture characterization (Bakulin et al., 2000).

ACKNOWLEDGMENTS

We are grateful to members of the A(nisotropy)-Team of the Center for Wave Phenomena (CWP), Colorado School of Mines, for helpful discussions and to Ken Larner (CSM), Joe Dellinger (BP), and the anonymous referees of Geophysics for their careful reviews of the manuscript. The support for this work was provided by the Consortium Project on Seismic Inverse Methods for Complex Structures at CWP and by the Chemical Sciences, Geosciences and Biosciences Division, Office of Basic Energy Sciences, U.S. Department of Energy.

REFERENCES

Alford, R. M., 1986, Shear data in the presence of azimuthal anisotropy: 56th Annual International Meeting, SEG, Expanded Abstracts, 476–479.

Alkhalifah, T., and I. Tsvankin, 1995, Velocity analysis in transversely isotropic media: Geophysics, **60**, 1550–1566.

Bakulin, A., V. Grechka, and I. Tsvankin, 2000, Estimation of fracture parameters from reflection seismic data—Part II: Fractured models with orthorhombic symmetry: Geophysics, **65**, 1803–1817.

Granli, J. R., B. Arntsen, A. Sollid, and E. Hilde, 1999, Imaging through gas-filled sediments using marine shear-wave data: Geophysics, **64**, 668–667.

Grechka, V., and P. Dewangan, 2003, Generation and processing of pseudo shear-wave data: Theory and case study: Geophysics, **68**, 1807–1816.

Grechka, V., and I. Tsvankin, 1998a, Feasibility of nonhyperbolic moveout inversion in transversely isotropic media: Geophysics, **63**, 957–969.

———, 1998b, 3-D description of normal moveout in anisotropic inhomogeneous media: Geophysics, **63**, 1079–1092.

———, 1999a, 3-D moveout velocity analysis and parameter estimation for orthorhombic media: Geophysics, **64**, 820–837.

———, 1999b, 3-D moveout inversion in azimuthally anisotropic media with lateral velocity variation: Theory and a case study: Geophysics, **64**, 1202–1218.

———, 2002, PP + PS = SS: Geophysics, **67**, 1961–1971.

Grechka, V., S. Theophanis, and I. Tsvankin, 1999, Joint inversion of P- and PS-waves in orthorhombic media: Theory and a physical-modeling study: Geophysics, **64**, 146–161.

Grechka, V., P. Contreras, and I. Tsvankin, 2000, Inversion of normal moveout for monoclinic media: Geophysical Prospecting, **48**, 577–602.

Grechka, V., A. Pech, and I. Tsvankin, 2002a, P-wave stacking-velocity tomography for VTI media: Geophysical Prospecting, **50**, 151–168.

———, 2002b, Multicomponent stacking-velocity tomography for transversely isotropic media: Geophysics, **67**, 1564–1574.

Grechka, V., I. Tsvankin, A. Bakulin, J. O. Hansen, and C. Signer, 2002c, Joint inversion of PP and PS reflection data for VTI media: A North Sea case study: Geophysics, **67**, 1382–1395.

Le Stunff, Y., V. Grechka, and I. Tsvankin, 2001, Depth-domain velocity analysis in VTI media using surface P-wave data: Is it feasible?: Geophysics, **66**, 897–903.

Obolentseva, I. R., and V. Grechka, 1989, Ray-tracing method in anisotropic media: Institute of Geology and Geophysics Press, Novossibirsk (in Russian).

Schoenberg, M., and K. Helbig, 1997, Orthorhombic media: Modeling elastic wave behavior in a vertically fractured earth: Geophysics, **62**, 1954–1974.

Thomsen, L., 1986, Weak elastic anisotropy: Geophysics, **51**, 1954–1966.

———, 1999, Converted-wave reflection seismology over inhomogeneous, anisotropic media: Geophysics, **64**, 678–690.

Tsvankin, I., 1997, Anisotropic parameters and P-wave velocity for orthorhombic media: Geophysics, **62**, 1292–1309.

———, 2001, Seismic signatures and analysis of reflection data in anisotropic media: Elsevier Science.

Tsvankin, I., and V. Grechka, 2000a, Dip moveout of converted waves and parameter estimation in transversely isotropic media: Geophysical Prospecting, **48**, 257–292.

———, 2000b, Two approaches to anisotropic velocity analysis of converted waves: 70th Annual International Meeting, SEG, Expanded Abstracts, 1193–1196.

Wild, P., and S. Crampin, 1991, The range of effects of azimuthal isotropy and EDA anisotropy in sedimentary basins: Geophysical Journal International, **107**, 513–529.